Adsorption of an Mn atom on a ZnO sheet and nanotube: a density functional theory study

2010 J. Phys.: Condens. Matter 22 175501

(http://iopscience.iop.org/0953-8984/22/17/175501)

J. Phys.: Condens. Matter **22** (2010) 175501 (7pp) doi:10.1088/0953-8984/22/17/175501

Adsorption of an Mn atom on a ZnO sheet and nanotube: a density functional theory study

A L He[1,2], X Q Wang[1], R Q Wu[2], Y H Lu[2] and Y P Feng[2]

[1] Department of Physics, Chongqing University, Chongqing 400030, People's Republic of China
[2] Department of Physics, National University of Singapore, 117542, Singapore

E-mail: xqwang@cqu.edu.cn and phyfyp@nus.edu.sg

Received 12 January 2010, in final form 15 March 2010
Published 7 April 2010
Online at stacks.iop.org/JPhysCM/22/175501

Abstract

First-principles calculations based on density functional theory were performed to study the stable geometries, electronic structure and magnetic properties of the adsorption of a single Mn atom on a graphitic ZnO sheet and a (9, 0) single-wall ZnO nanotube. For the graphitic ZnO sheet, the Mn atom prefers to reside above the center of a hexagon (H site), with a relatively large binding energy of 1.24 eV. The H site is also the most stable site for adsorption of an Mn atom inside the ZnO nanotube, with a large binding energy of 1.47 eV. In both of these cases, the total magnetic moment is 5.0 μ_B per Mn atom, which is the same as that of a free Mn atom. When the Mn atom is adsorbed outside the tube, the most energetically favorable site is the atop oxygen site. The magnetic moment is 3.19 μ_B for this configuration. The smaller magnetic moment is mainly due to the strong p–d mixing of O and Mn orbitals. The different adsorption behaviors are related to the curvatures of the nanostructures.

(Some figures in this article are in colour only in the electronic version)

1. Introduction

Single-wall nanotubes represent a unique class of materials in which all atoms are located at the surface. Since electrons flowing through such nanotubes are confined in the surface, nanotubes are attractive for sensing biological and chemical molecules. In addition, their tubular structures enable nanofluidic devices that are useful for novel sensing applications. Besides carbon and boron nitride nanotubes [1], many other nanotubes such as TiO_2 [2], GaN [3], silica [4] and ZnO [5, 6] nanotubes have been synthesized by using a multi-step process with templates or by hydrothermal techniques. Of these materials, ZnO nanotubes (ZnONTs) stand out due to their multifunctional properties for optical, electronic and piezoelectric applications. ZnONTs are expected to accomplish many applications at the cutting edge of nanotechnology.

In contrast to the large amount of experimental investigations, only a few theoretical studies on the nanostructural ZnO have been carried out so far. Several synthetic routes have yielded multi-walled ZnO nanotubes [7–14], which are 20–450 nm in diameter and have wall thicknesses of 4–100 nm. The stability and the electronic structure of single-walled ZnO nanotubes (SWZnONTs) have been studied theoretically [15–20]. Tu *et al* demonstrated the existence of single-wall ZnO nanotubes by first-principles calculations and proposed that they might be synthesized by the solid–vapor phase process with carbon nanotubes as templates [15]. Wang *et al* found that finite tubular structures, $(ZnO)_n$, are metastable for $n = 9$–18 and suggested that ZnO nanotubes resemble C or BN nanotubes [16]. Xu *et al* [19] showed that all SWZnONTs are direct bandgap semiconductors with relatively uniform bandgaps. Erkoc *et al* applied semiempirical molecular orbital self-consistent field calculations to study the structural and electronic properties of armchair and zigzag models of single-wall ZnO nanotubes [21]. Even though the single-wall tubular form of ZnO has not been synthesized experimentally, it was found that ZnO can exist in many different forms, including nanowalls [22, 23], One can expect that ZnO sheets and nanotubes could be produced via the current methods using

transition metal (TM) atoms as catalysts [24]. Therefore, we believe it is important to understand the effect of the adsorption of TM atoms on the ZnO nanotubes.

At the same time, functionalization of nanotubes through decorations with atoms and/or molecules is an effective way to modify their physical properties. Manganese oxide exhibited higher catalytic activity for the low-temperature catalytic combustion than Fe or Co oxides [25], so in this work we investigate the interaction of an Mn atom with a (9, 0) single-wall ZnO nanotube and with a graphitic ZnO sheet by first-principles spin-polarized calculations based on density functional theory (DFT). The computational details are given in section 2. In section 3, we first discuss adsorption of a single Mn atom on the graphitic ZnO sheet. Results of binding energies, electronic structures and magnetic properties corresponding to various binding sites are presented. Following that, the adsorption of a single Mn atom at various sites on the outer and inner walls of the (9, 0) zigzag single-wall ZnO nanotube are discussed, respectively. In each case, the structural, electronic and magnetic properties of the Mn-doped (9, 0) single-wall ZnO nanotube are analyzed. A conclusion is given in section 4.

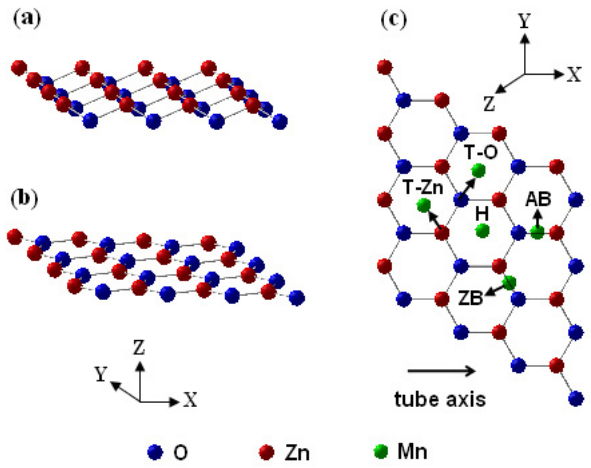

Figure 1. The structure of the graphitic ZnO sheet: (a) unrelaxed, (b) relaxed and (c) various adsorption sites for a single Mn atom on the graphitic ZnO sheet and the (9, 0) ZnO nanotube. H denotes an Mn over the center of a hexagon. T–O and T–Zn represent Mn on top of an oxygen and a Zn atom, respectively. AB and ZB indicate the bridge sites, over an axial Zn–O and zigzag Zn–O bond, respectively. For the ZnO sheet, the axial and zigzag sites are equivalent, namely AB $\Leftrightarrow$ ZB $\Leftrightarrow$ B.

2. Computational method

Our calculations were performed using a first-principles method based on the density functional theory (DFT) [26] within the generalized gradient approximation (GGA) [27] as implemented in the Vienna *ab initio* simulation package (VASP) [28]. The projector-augmented plane wave (PAW) [29] potentials were used to represent the electron–ion interactions. A kinetic energy cutoff of 520 eV was used to ensure a convergence better than 1 meV per atom for total energy.

A (0001) layer of ZnO cleaved from bulk ZnO [18] was taken as the initial structure of the graphitic ZnO sheet. The surface model is periodic in the ZnO layer (figure 1(a)). The graphitic ZnO sheet was modeled using a 2×2 unit cell containing 32 atoms, with a vacuum region of 15 Å thick, in the calculations. A Γ-centered $2\times2\times2$ k-mesh was used to sample the irreducible Brillouin zone in our calculation. The structure is fully relaxed using the conjugate gradient algorithm [30]. The optimized lattice constant of the single ZnO sheet is 6.50 Å within the GGA.

The minimum energy structure after relaxation changed from a rippled surface to a flat sheet, in which all of the Zn and O atoms are in the same atomic plane (figure 1(b)). The Zn–O bond length decreased from 2.01 Å in bulk ZnO to 1.876 Å, which is in good agreement with results of a recent theoretical study [18]. The calculated cohesive energy of the graphitic ZnO is -7.02 eV which is slightly larger than that reported by Zhu *et al* (-7.25 eV) using DMol [31], which is likely due to the different computational methods. The pure ZnO sheet has a direct bandgap of 1.69 eV at the Γ-point, which is very close to the value (1.68 eV) reported by Xu *et al* [19].

Earlier DFT calculations showed that zigzag ZnO nanotubes are more stable than the armchair nanotubes [18]. Therefore, in this study, we consider only the single-wall zigzag (9, 0) ZnO nanotube in our study of Mn-doped ZnO nanotubes. To minimize the interaction between Mn atoms in neighboring cells, a supercell which is two units long in the direction of the tube axis, i.e. 11.32 Å, was used in this work. The resulting supercell contains 36 formula units of ZnO ($Zn_{36}O_{36}$). A vacuum layer of 15 Å between the nanotube and its images in neighboring cells was used to ensure negligible interactions between them. A Γ-centered $1\times1\times2$ k-mesh was used to sample the irreducible Brillouin zone. All structures were fully optimized using the conjugate gradient method until the Hellmann–Feynman forces were less than 0.05 eV Å^{-1}. Compared to a carbon nanotube, the optimized ZnO nanotubes were distorted in which zinc and oxygen atoms were shifted inward and outward radially, respectively, forming coaxial cylinders of different diameters (D_{Zn} = 9.28 Å and D_O = 9.48 Å). The diameter of the oxygen cylinder is larger than that of zinc and their difference is 0.20 Å. The Zn–O bond lengths vary from 1.899 to 1.904 Å, which are noticeably shorter than the corresponding bond length in bulk ZnO (2.01 Å), but are larger than that in graphitic ZnO (1.876 Å), and similar to those of BN and GaN nanotubes [32, 33]. We also calculated the bandgap of a pure (9, 0) ZnO nanotube which is 1.640 eV at the Γ-point. This is in excellent agreement with the value reported by Xu *et al* [19], who found a bandgap of 1.641 eV at the Γ-point.

3. Results and discussion

There are four possible adsorption sites for a single Mn atom on the graphitic ZnO sheet (figure 1(c)): (i) over the center of a hexagon (H in figure 1), (ii) over an oxygen atom (T–O site), (iii) over a Zn atom (T–Zn site) and (iv) at the bridge site over a Zn–O bond (B site). (For the ZnO sheet, the axial and zigzag bridge sites are equivalent.)

Table 1. The calculated binding energies (E_b) and magnetic moments (μ) for different adsorption sites of a single Mn atom on a graphitic ZnO sheet and a (9, 0) ZnO nanotube, respectively.

System	Site	E_b (eV)	μ (μ_B)
ZnO sheet	H	1.24	5.00
	T–O	1.14	5.00
	B	1.12	5.00
	T–Zn	0.34	5.00
Outer wall of (9, 0) nanotube	T–O	0.63	3.19
	T–Zn	0.63	3.19
	AB	0.63	3.19
	ZB	0.62	3.22
	H	0.60	3.31
Inner wall of (9, 0) nanotube	H	1.47	5.00
	T–Zn	1.47	5.00
	T–O	0.69	5.00
	AB	0.69	5.00
	ZB	0.69	5.00
	Center	−0.25	5.00

For the (9, 0) ZnO nanotube, a Zn–O bond can be oriented either along the direction of the tube axis (axial direction) or along the zigzag lines around the tube (zigzag direction). Here AB and ZB indicate the bridge sites over an axial Zn–O and zigzag Zn–O bond, respectively. As in the case of a graphitic ZnO sheet, H also refers to the adsorption site of a single Mn atom over the center of a hexagon, T–O corresponds to the adsorption site atop an O atom and T–Zn represents the configuration of an Mn atom atop a Zn atom. Since the ZnO tube has two surfaces, inside and outside, adsorption on both surfaces were considered. The various different adsorption sites are shown in figure 1(c).

To compare the relative stability of different adsorption sites, we calculated the binding energy (E_b) which is defined as

$$E_b = E(\text{pure}) + E(\text{Mn}) - E(\text{Mn-doped}) \quad (1)$$

where E(pure) is the total energy of the undoped system (the pure ZnO sheet or the pure ZnO nanotube), E(Mn) is the spin-polarized total energy of an Mn atom in the $3d^5 4s^2$ ground state configuration and E(Mn-doped) is the spin-polarized total energy of the optimized structure of the Mn-doped system (the Mn-doped ZnO sheet or the Mn-doped ZnO nanotube). The calculated binding energies and magnetic moments, using the fully relaxed structures, are tabulated in table 1 for each adsorption site.

3.1. Interaction of Mn with the graphitic ZnO sheet

As shown in table 1, the H site was found to be most stable among the various adsorption sites considered for the graphitic ZnO sheet, with a binding energy of 1.24 eV. In the optimized structure, the position of Mn is 1.73 Å above the ZnO sheet and its three neighboring oxygen atoms are all relaxed towards the Mn atom by about 0.51 Å, resulting in the formation of three Mn–O bonds. The average distance between the Mn and O, however, is 2.11 Å, which is larger than the length of the Zn–O bond (1.89 Å) in the graphitic ZnO sheet. This indicates that the interaction between Mn and O is weak, possibly due to the half-filled 3d electronic shell and filled 4s of the Mn atom [34].

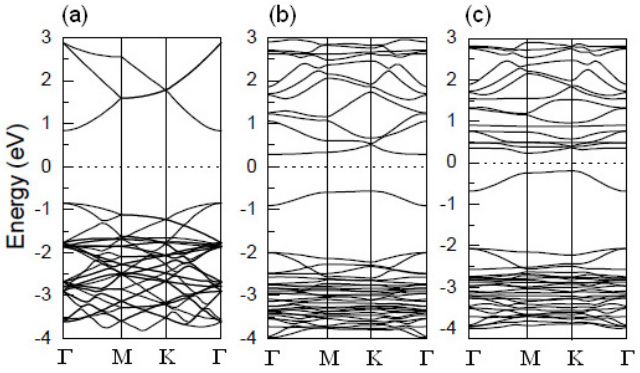

Figure 2. Band structures of (a) the pristine graphitic ZnO sheet, (b) the majority spin and (c) the minority spin for Mn adsorption at the H site on the ZnO sheet. The Fermi level is set to zero.

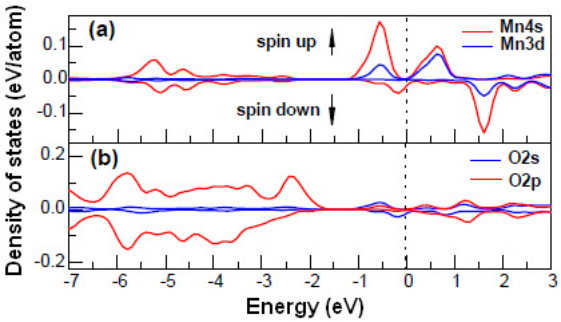

Figure 3. Projections of local density of states onto (a) the Mn 3d and 4s orbitals, and (b) the O 2s and 2p orbitals for Mn adsorption at the H site on ZnO sheet. Atoms Mn, O and Zn are labeled in figure 1(c).

In figures 2 and 3, the band structures and local density of states (LDOS) for the H configuration of the Mn-doped ZnO sheet are shown, respectively. The band structure of the pristine graphitic ZnO sheet is also shown in figure 2(a) for comparison. We can see that all states are in twofold degeneracy, indicating no spin polarization in the pristine graphitic ZnO sheet, similar to that of the pristine BN sheet [35]. In the majority spin bands (figure 2(b)) of the Mn-doped ZnO sheet, four flat bands are located between 2.6 and 3.0 eV below the Fermi level, which are mainly contributed by the 4s orbitals of Mn and 2p orbitals of oxygen. The first band below the Fermi level corresponds to Mn 4s orbitals and oxygen 2s orbitals, as can be seen from the LDOS (figure 3). On the other hand, in the minority spin bands (figure 2(c)), we can see that those bands below −2.0 eV are very similar to those of the majority spin. However, the first band below the Fermi level is closer to the Fermi level than that of the majority spin. Two nearly flat bands appear at 0.5 eV and 0.9 eV above the Fermi level, respectively, which are due to the mixture of the Mn 4s and oxygen 2p orbitals. The total magnetic moment per Mn atom of the Mn-doped graphitic ZnO sheet is almost the same as that of a free Mn atom. Projection of the magnetic moment onto the atomic sites showed that three nearest-neighbor oxygens of Mn contribute about 0.1 μ_B to the total magnetic moment. A Mulliken charge analysis indicated

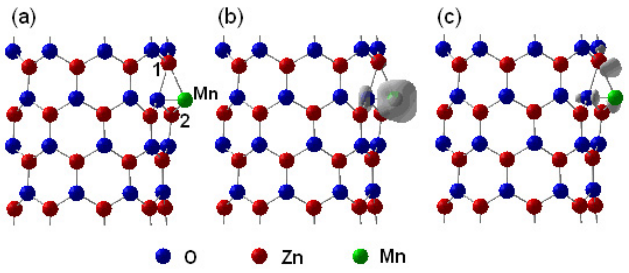

Figure 4. (a) The relaxed structure of the ZnO nanotube with an Mn atom adsorbed at the T–O site on the outer wall of the (9, 0) ZnO nanotube. The spin density isosurfaces correspond to (b) 0.022 e Å^{-3} and (c) -0.020 e Å^{-3} for the same configuration.

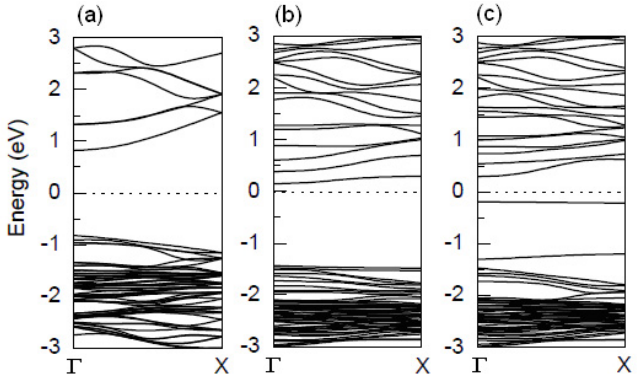

Figure 5. Band structures of (a) the pure (9, 0) ZnO nanotube, (b) the majority spin and (c) the minority spin for Mn adsorption at the T–O site on the outer wall of the (9, 0) ZnO nanotube. The Fermi level is set to zero.

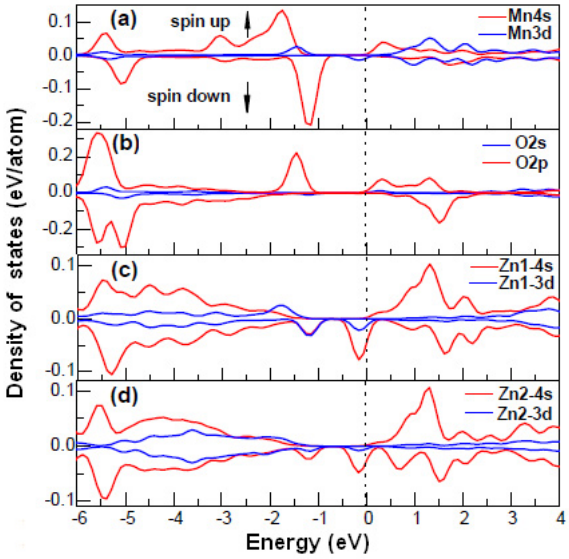

Figure 6. Projections of local density of states onto (a) the Mn 3d and 4s orbitals, (b) the 2s and 2p orbitals of O, (c) the 3d and 4s orbitals of Zn atom 1 and (d) the 3d and 4s orbitals of Zn atom 2, for Mn adsorption at the T–O site on the outer wall of the (9, 0) ZnO nanotube. Zn atoms 1 and 2 are shown in figure 4(a).

that there is a small charge transfer from the O 2p orbital to the 3d orbital of Mn.

In addition to the H site, other configurations, such as the T–O site, which is the second most stable configuration, has a binding energy of 1.14 eV, only 0.1 eV smaller than that of the most stable H site. In the relaxed T–O configuration, the distance between the Mn and the oxygen atom is 1.98 Å. The total magnetic moment of the T–O configuration is the same as that of the H configuration. The bridge site (AB or ZB in figure 1(c)) was found unstable and transformed into the T–O configuration after structural relaxation. T–Zn was found the least stable site, as indicated by the smallest binding energy in table 1. In the optimized T–Zn configuration, the distance between the Mn atom and the Zn atom underneath is 2.71 Å, which is larger than the summation of the covalent radii of the Mn atom (1.39 Å) and Zn atom (1.31 Å). The lower binding energy (0.34 eV) implies that the Mn atom is physisorbed on the ZnO sheet. As a result, the magnetic moment of the Mn-doped system in this configurations is exactly the same as that of a free Mn atom. A detailed analysis was done for the T–Zn site and the results showed that the effective electronic configurations of the Mn atom in the T–Zn site are close to $3d^7 4s^0$. The low binding energy of this configuration could be due to the high energy penalty for promoting the 4s orbital to the 3d orbital [24].

3.2. Adsorption of Mn to the outer wall of (9, 0) ZnO nanotube

For adsorption of an Mn atom on the outer wall of the (9, 0) nanotube, the T–O site was found energetically most favorable, with a binding energy of 0.63 eV. In the relaxed T–O configuration (figure 4(a)), the Mn atom pushed the oxygen atom below inward by 0.38 Å from its position in the pure ZnO tube. The distance between the Mn atom and the neighboring oxygen atom is 1.70 Å, which is smaller than that in the T–O configuration of the Mn-doped ZnO sheet (1.98 Å). The calculated band structure and LDOS for the T–O configuration are shown in figures 5 and 6, respectively. The energy band diagram of the pure (9, 0) ZnO tube is also shown in figure 5(a) for comparison. In the majority spin bands (figure 5(b)), two Mn 3d bands are clearly visible between 1.3 and 1.5 eV below the Fermi level and two Mn 4s band lie between 1.9 and 2.0 eV below the Fermi level. However, in the minority spin bands (figure 5(c)), one Mn 4s band lies at 0.2 eV below the Fermi level and one Mn 3d band lies at 1.3 eV below the Fermi level. Figure 4(b) shows the spin density isosurface corresponding to 0.02 e Å^{-3} for the T–O configuration of the Mn-doped (9, 0) ZnO tube. It shows that the oxygen atom next to Mn (figure 4(a)) carries a finite positive spin density. The local magnetic moment of 0.04 μ_B is due to oxygen 2p orbitals. In contrast, the two Zn atoms which are nearest neighbors of Mn (atoms 1 and 2 in figure 4(a)) have negative spin densities, with -0.05 μ_B and -0.03 μ_B local magnetic moments, respectively, as shown in figure 4(c). The negative local magnetic moment comes mainly from Zn 4s orbitals, as clearly shown by the LDOS in figures 6(c) and (d).

It is interesting to note that, for the optimized T–Zn configuration, the Mn atom moved from the top of Zn to the

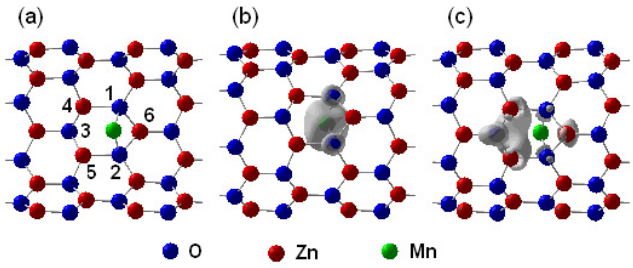

Figure 7. (a) The relaxed structure of the ZnO nanotube with an Mn atom adsorbed at the H site on the inner wall of the (9, 0) ZnO nanotube. The spin density isosurfaces correspond to (b) 0.03 e Å^{-3} and (c) -0.002 e Å^{-3} for the same configuration.

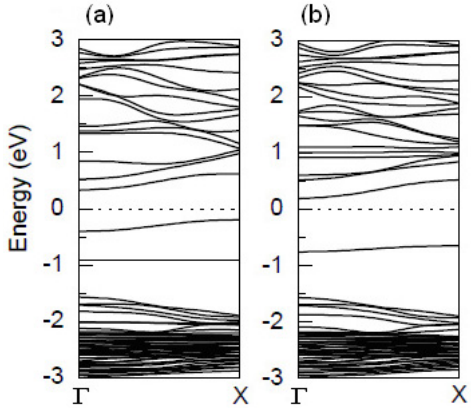

Figure 8. Band structures of (a) the majority spin and (b) the minority spin for an Mn adsorbed at the H site on the inner wall of the (9, 0) ZnO nanotube. The Fermi level is set to zero.

top of oxygen. The distances from the Mn atom to the oxygen atom and its two nearest-neighboring Zn atoms (atoms 1 and 2 in figure 4(a)) are 1.70 Å, 2.43 Å and 2.45 Å, respectively. This is essentially the T–O configuration. The calculated binding energies and magnetic moments of the T–Zn and T–O configurations are also the same, as indicated in table 1. The two initial configurations in which the Mn atom was at the bridge sites over a Zn–O bond, AB and ZB, also relaxed to the same T–O structure. During structural relaxation, the Mn atom moved to the top of oxygen from the bridge site, The final configurations share the same binding energy of 0.62 eV and the magnetic moment of 3.22 μ_B. Finally for the H adsorption site, the structure also relaxes to the same geometry, with the final position of Mn over the O. Therefore, for adsorption of an Mn atom on the outer wall of the (9, 0) ZnO nanotube, the atop oxygen site seems exceptionally stable. The Mn atom tends to move to the top of the oxygen atom so that it can form bonds with this oxygen and the two nearest-neighboring Zn atoms. We notice that the magnetic moments are lower for adsorption of Mn on the outer wall of the ZnO nanotube than Mn on the ZnO sheet and on the inner wall of the nanotube, as listed in table 1. The reason for the low magnetic moments is because the Mn atom is chemisorbed on the ZnO nanotube and local magnetic moments from Zn atoms in opposite directions partially cancel that of Mn.

3.3. Adsorption of Mn to the inner wall of (9, 0) ZnO nanotube

For adsorption of Mn on the inside wall of the nanotube, it is found that, among all adsorption sites considered, the relaxed H configuration is the most stable structure, with a binding energy of 1.47 eV. We take note that the T–Zn configuration also transforms into the same final configuration upon structural relaxation. Therefore, the T–Zn site is not a stable adsorption site for Mn on the inside wall of the (9, 0) ZnO nanotube. It is interesting to note that both AB and ZB relax to the T–O configuration. It is less stable compared to the H site, with a lower binding energy of 0.69 eV. The distance between the Mn atom and oxygen atom in the relaxed structure is 1.76 Å, which is larger than the bond length of 1.70 Å when Mn is adsorbed at the T–O site of the outer wall of the nanotube, but lower than the value of 1.98 Å in the same configuration of the ZnO sheet. However, when the Mn atom is located in the center of the tube (center site in table 1), although the initial configuration has little change after relaxation, the binding energy of -0.25 eV indicates that this site is energetically unfavored for Mn adsorption. In this case, the Mn atom will not form bonds with any atom. As a result, the magnetic moment (5.0 μ_B) of the Mn-doped system in this configuration is exactly the same as that of a free Mn atom.

The optimized structure of the most stable configuration for Mn adsorption on the inner wall of the nanotube (H site) is shown in figure 7(a). The distances between the Mn atom and two closest oxygen atoms (atom 1 and atom 2 in figure 7(a)) are 1.852 Å and 1.856 Å, respectively. The third oxygen (atom 3 in figure 7(a)), however, was pushed away by the Mn atom and the distance between them became 3.46 Å from the initial 2.17 Å. The three Zn atoms (atom 4, atom 5 and atom 6 in figure 7(a)), which are near to the Mn atom, are also pushed away by the Mn atom, and the final distances between the Mn atom and Zn atoms 4 and 5 are both 2.60 Å, while that between the Mn atom and Zn atom 6 is 2.62 Å.

The calculated band structure and LDOS for the H configuration are shown in figures 8 and 9, respectively. In the band structure of majority spin (figure 8(a)), one oxygen 2p band is clearly seen at 0.9 eV below the Fermi level. Another band is located between 0.2 and 0.4 eV below the Fermi level, which corresponds to the Mn 4s orbital and oxygen (atom 2) 2p orbital, as can be seen from the LDOS (figure 9). On the other hand, in the minority spin bands (figure 8(b)), one band appears at 0.75 eV below the Fermi level, which is mainly contributed by the 4s orbital of Mn. Figure 7(b) shows the spin density isosurface corresponding to 0.03 e Å^{-3} for the H configuration of an Mn-doped (9, 0) ZnO tube. It shows that oxygen atoms 1 and 2 (figure 7(a)) bonded to the Mn atom have finite positive spin densities, with 0.076 and 0.077 μ_B local magnetic moments, respectively. In contrast, the two Zn atoms (Zn atoms 3 and 4), which are nearest neighbors of Mn, and oxygen atom 3 (figure 7(a)) have negative spin densities, with -0.005, -0.005 and -0.025 μ_B local magnetic moments, respectively, as shown in figure 7(c). It is noted that the local magnetic moment of oxygen atom 3 is larger than that of Zn atoms 4 and 5 (-0.005 μ_B), which comes mainly from its 2p

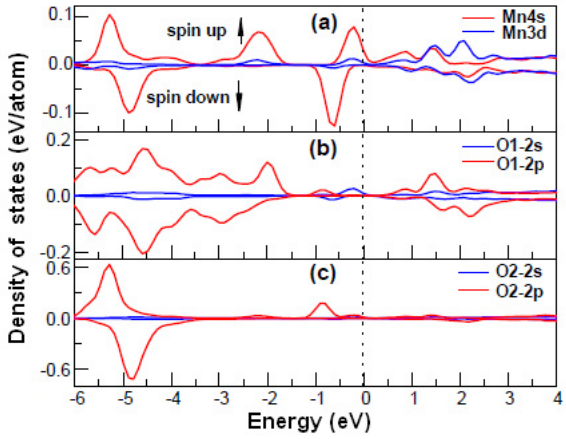

Figure 9. Projections of local density of states onto (a) the Mn 3d and 4s orbitals, (b) the 2s and 2p orbitals of O atom 1 and (c) the 2s and 2p orbitals of O atom 2 for Mn adsorption at the H site on the inner wall of the (9, 0) ZnO nanotube. O atoms 1 and 2 are shown in figure 7(a).

orbitals, as clearly shown by the LDOS (figure 9(c)). The local magnetic moment of the Mn atom is 3.94 μ_B. Contributions from all atoms result in a total magnetic moment of 5.0 μ_B for the Mn-doped tube system.

3.4. Curvature effect

The differences between the graphitic ZnO sheet and a ZnO nanotube, and between the inner and outer walls of a ZnO nanotube, are in their curvatures. The different adsorption behaviors of Mn on the graphitic ZnO sheet and on the inner and outer walls of a ZnO nanotube could be related to partial sp^3 hybridization of the electronic orbitals in the ZnO nanotube due to the curvature effects. The hybridization of the d-electron states of Mn with the s- and p-electron states of the O atoms is enhanced when the supporting ZnO nanotubes have large curvatures. For adsorption of an Mn atom on the outer wall of the (9, 0) nanotube, the curvature of the ZnO nanotube is negative. The Mn atom prefers to reside on the top of an O atom and form bonds with this O and its two nearest-neighboring Zn atoms. This configuration favors charge transfer from O 2p and Zn 3d states to 3d orbitals of the Mn atom, as confirmed by Mulliken population analysis. The large charge transfer leads to a lower magnetic moment, compared to that when Mn is adsorbed on the inner wall of the ZnO nanotube or on the graphitic ZnO sheet. The curvature of the graphitic ZnO sheet is zero. When the Mn atom is adsorbed on the graphitic ZnO sheet, it energetically favors the H site in which the Mn atom forms bonds with three O atoms. Charge transfer from the oxygen atoms to the Mn atom, and bonding between Mn and the graphitic sheet, are maximized in such a configuration. As discussed above, H is also the most stable configuration for adsorption of Mn atoms on the inner wall of the nanotube. Due to the positive curvature of the nanotube, the Mn atom bonds only to two O atoms, and the direction of charge transfer is reversed, so the Mn atom donates charges to the nanotube. Because a concave surface enhances its interaction with the Mn atom, the binding energy of Mn is the largest when it is adsorbed on the inner wall of the nanotube while it is the least when it is adsorbed on the outer wall of the nanotube.

4. Conclusion

The absorption of an Mn atom on a graphitic ZnO sheet and a single-wall zigzag (9, 0) ZnO nanotube are studied by *ab initio* calculations. For the Mn-doped ZnO sheet, the most stable adsorption site is the H site. The Mn atom tends to push its three nearest-neighbor Zn atoms out of the plane so that it can form bonds with its three nearest-neighbor oxygen atoms. Similarly, the H configuration is also the most energetically favorable site for adsorption of a single Mn atom on the inner wall of the (9, 0) ZnO nanotube. For this configuration, the binding energy is 1.47 eV, which is the largest among all adsorption sites. In this case, the Mn atom pushes one of the three nearest oxygen atoms away and only form bonds with the other two neighboring oxygen atoms. The average Mn–O bond length is 1.85 Å. The total magnetic moment when Mn is adsorbed either on the graphitic ZnO sheet or on the inner wall of the (9, 0) ZnO nanotube is the same as that of a free Mn atom. When the Mn atom is adsorbed on the outer wall of the (9, 0) ZnO nanotube, however, the most energetically favorable site is the T–O site. All other adsorption sites considered are energetically not favored and transform to the T–O site upon structural relaxation. The Mn atom prefers to bond with the oxygen atom underneath it and with its two nearest-neighbor Zn atoms. The strong p–d mixing of O and Mn leads to a low magnetic moment of 3.19 μ_B, which is different from absorption of Mn on the ZnO sheet and on the inner wall of the ZnO nanotube. The present study provides some useful reference to the synthesis of ZnO nanotubes using TM atoms as catalysts and its potential applications.

Acknowledgments

This work was supported by the National Research Foundation (Singapore) Competitive Research Program (grant no. NRF-G-CRP 2007-05). Part of the work was carried out using the computing facility at the Computer Center of the National University of Singapore. We would also like to thank the China Scholarship Council (CSC) for partially supporting the joint-training research in Singapore.

References

[1] Iijima S 1991 *Nature* **354** 56
[2] Mor G K, Shankar K, Paulose M, Varghese O K and Grimes C A 2005 *Nano Lett.* **5** 191
[3] Goldberger J, He R R, Zhang Y F, Lee S, Yan H Q, Choi H and Yang P D 2003 *Nature* **422** 599
[4] Fan R, Wu Y Y, Li D Y, Yue M, Majumdar A and Yang P D 2003 *J. Am. Chem. Soc.* **125** 5254
[5] Sun Y, Fuge G M, Fox N A, Riley D J and Ashfold M N R 2005 *Adv. Mater.* **17** 2477
[6] Wu G S, Xie T, Yuan X Y, Li Y, Yang L, Xiao Y H and Zhang L D 2005 *Solid State Commun.* **134** 485

[7] Zhang J, Sun L, Liao C and Yan C 2002 *Chem. Commun.* **3** 262
[8] Wu J J, Liu S C, Wu C T, Chen K H and Chen L C 2002 *Appl. Phys. Lett.* **81** 1312
[9] Hu J Q, Li Q, Meng X M, Lee C S and Lee S T 2003 *Chem. Mater.* **15** 305
[10] Zhang X H, Xie S Y, Jiang Z Y, Zhang X, Tian Z Q, Xie Z X, Huang R B and Zheng L S 2003 *J. Phys. Chem.* B **107** 10114
[11] Xing Y J, Xi Z H, Xue Z Q, Zhang X D, Song J H, Wang R M, Xu J, Song Y, Zhang S L and Yu D P 2003 *Appl. Phys. Lett.* **83** 1689
[12] Kong X H, Sun X M, Li X L and Li Y D 2003 *Mater. Chem. Phys.* **82** 997
[13] Kong X Y, Ding Y and Wang Z L 2004 *J. Phys. Chem.* B **108** 570
[14] Sun Y, Fuge G M, Fox N A, Riley D J and Ashfold M N R 2005 *Adv. Mater.* **17** 2477
[15] Tu Z C and Hu X 2006 *Phys. Rev.* B **74** 035434
[16] Wang B L, Nagase S, Zhao J J and Wang G H J 2007 *Phys. Chem.* C **111** 4956
[17] Shen X P, Allen B, Muckerman J T, Davenport J W and Zheng J C 2007 *Nano Lett.* **7** 2267
[18] Wang B L, Nagase S, Zhao J J and Wang G H 2007 *Nanotechnology* **18** 345706
[19] Xu H, Zhang R Q, Zhang X, Rosa A L and Frauenheim T 2007 *Nanotechnology* **18** 485713
[20] Yang Y R, Yan X H, Xiao Y and Guo Z H 2007 *Chem. Phys. Lett.* **446** 98
[21] Erkoc S and Kokten H 2005 *Physica* E **28** 162
[22] Maeng J, Jo G, Choe M, Park W, Kwon M, Park S and Lee T 2009 *Thin Solid Films* **518** 865
[23] In S K, Do Y K, In J K and Se Y C 2009 *Japan. J. Appl. Phys.* **48** 08HJ02
[24] Peng G W, Feng Y P and Huan A C H 2006 *Phys. Rev.* B **73** 155429
[25] Zeynep Ö, Gülin S, Pozan S and İsmail B 2009 *Chem. Eng. J.* **155** 94
[26] Kohn W and Sham L J 1965 *Phys. Rev.* **140** A1133
[27] Wang Y and Perdew J P 1991 *Phys. Rev.* B **44** 13298
[28] Kresse G and Furthmüller J 1996 *Phys. Rev.* B **54** 11169
[29] Kresse G and Joubert D 1999 *Phys. Rev.* B **59** 1758
[30] Press W H, Flannery B P, Teukolsky S A and Vetterling W T 1986 *New Numerical Recipes* (New York: Cambridge University Press)
[31] Zhu Z G, Chutia A, Sahnoun R, Koyama M, Tsuboi H, Hatakeyama N, Endou A, Takaba H, Kubo M, Carpio C D and Miyamoto A 2002 *Japan. J. Appl. Phys.* **41** 2410
[32] Lee S M, Lee Y H, Hwang Y G, Elsner J, Porezag D and Frauenheim T 1999 *Phys. Rev.* B **60** 7788
[33] Hernandez E, Goze C, Bernier P and Rubio A 1998 *Phys. Rev. Lett.* **80** 4502
[34] Wang Q, Sun Q, Jena P and Kawazoe Y 2009 *Phys. Rev.* B **79** 115407
[35] Wu R Q, Peng G W, Liu L and Feng Y P 2006 *J. Phys.: Condens. Matter* **18** 569